

Contents lists available at ScienceDirect

### Transportation Research Part C

journal homepage: www.elsevier.com/locate/trc



## Design and field evaluation of cooperative adaptive cruise control with unconnected vehicle in the loop



Daegyu Lee <sup>a</sup>, Seungwook Lee <sup>a</sup>, Zheng Chen <sup>b,\*</sup>, B. Brian Park <sup>c</sup>, David Hyunchul Shim <sup>a</sup>

- <sup>a</sup> Department of Electrical Engineering, KAIST, Daejeon 34141, Republic of Korea
- <sup>b</sup> PCI Technology Group CO., LTD, Guangzhou 510653, China
- <sup>c</sup> Link Lab & Department of Engineering Systems and Environment, University of Virginia, Charlottesville, VA, United States

#### ARTICLE INFO

# Keyword: Cooperative automated driving Mixed traffic CACC Unconnected vehicle Field test

#### ABSTRACT

To fully harvest the benefits of vehicular automation and connectivity in the mixed traffic, a cooperative longitudinal control strategy named Cooperative Adaptive Cruise Control with Unconnected vehicle in the loop (CACCu) has been proposed. When encountering an unconnected preceding vehicle, CACCu enables a Connected and Automated Vehicle (CAV) to benefit from communicating with a connected vehicle further ahead, rather than completely falling back to Adaptive Cruise Control (ACC). To validate the feasibility of CACCu, this study developed and tested a CACCu system with real vehicles in the field. A speed-command-based CACCu controller is designed and parameterized for optimizing the anticipated string stability. The experiment was conducted with two automated vehicles equipped with Mobileye sensors and Wi-Fi modules. The car-following performance of CACCu, in comparison with ACC and human driving (as the ego vehicle), was evaluated in the real-traffic scenarios constructed using NGSIM vehicle trajectory data. Over the 6 test runs for each control method, it was found that CACCu reduced 10.8% acceleration Root Mean Square (RMS), 60.8% spacing error RMS and 6.2% fuel consumption from ACC's, indicating advantages of CACCu in control accuracy, ride comfort and energy efficiency. Compared with human driving, CACCu also reduced 17.6% acceleration and 13.4% fuel consumption. More importantly, the CACCu was able to efficiently avoid the traffic disturbance amplifications that frequently happened to ACC and human driving, which means the string stability has been significantly improved by the CACCu.

#### 1. Introduction

In order to improve traffic safety and mobility, advanced technologies have been introduced and implemented through Intelligent Transportation Systems (ITS). Connected Automated Vehicle (CAV), which enables a variety of cooperative automated driving applications (Shladover, 2018), is expected to play a key role in ITS. One promising CAV application is Cooperative Adaptive Cruise Control (CACC) (Naus et al., 2010), which is developed from Adaptive Cruise Control (ACC). In addition to measuring the position of the preceding vehicle by onboard sensor, the Vehicle-to-Vehicle (V2V) communications enables CACC vehicles to immediately obtain

E-mail addresses: lee.dk@kaist.ac.kr (D. Lee), seungwook1024@kaist.ac.kr (S. Lee), zc4ac@virginia.edu (Z. Chen), bp6v@virginia.edu (B.B. Park), hcshim@kaist.ac.kr (D.H. Shim).

<sup>\*</sup> Corresponding author.

the traffic situation in the downstream, which helps improve the precision of longitudinal motion control (Milanes et al., 2014). As a result, the equipped vehicles can maintain short inter-vehicle headways (e.g., 0.6 s) with guaranteed safety and "string stability."

String stability (Naus et al., 2010) refers to the vehicle's capability of attenuating traffic disturbance from downstream, and keeping the vehicle string undisrupted by sudden acceleration or deceleration of any vehicles ahead of the platoon. In string-unstable situations, the speed/spacing disturbance from the preceding vehicle is amplified by the following vehicles, causing shockwaves along the traffic. It has been pointed out that the string-unstable dynamics of human-driven vehicles is an origin of the traffic jams that occur without apparent external reason (Sugiyama et al., 2008). Such disruptive behaviors were also observed on the existing commercial ACC systems (Gunter et al., 2020). Therefore, the string stability, which is hard to achieve in short headways for human driver or ACC, has become a design requirement (van Nunen et al., 2012) and also a basis for the various benefits of CACC. Previous studies have indicated that CACC can significantly improve roadway capacity (Liu et al., 2018), traffic flow quality (Van Arem et al., 2006) and energy efficiency (Shladover, 2018).

In despite of the great potentials, the usability of CACC may be seriously limited in the near future when the CAVs are mixed with a large number of non-CAVs. Although governments and manufacturers worldwide are making efforts to promote vehicular connectivity (Masini et al., 2018), CAVs are not likely to gain a dominant Market Penetration Rate (MPR) in the next two decades (Bansal and Kockelman, 2017). Consequently, the chance is rare to make CAVs travel consecutively in the mixed traffic. As most of the existing CACC systems require the connection with the nearest preceding vehicle (Naus et al., 2010; Milanes et al., 2014; van Nunen et al., 2012; Rajamani and Shladover, 2001; Ploeg et al., 2011), the CACC vehicle would have to degrade into ACC mode when its preceding vehicle is an unconnected vehicle.

There have been a few research efforts trying to address this issue of CACC. Graceful degradation of CACC (dCACC) (Ploeg et al., 2015) proposed to estimate preceding vehicle's acceleration using onboard radar if it is not obtainable via communication. It was proven that with proper tuning of the state estimator (Kalman filter), dCACC can fulfill string stability at a short time gap which is less than a half of that needed for ACC. Nevertheless, it turned out that the noise in the radar-measured acceleration could compromise the smoothness of vehicle trajectory and the ride comfort (Ploeg et al., 2015). A class of methods called Connected Cruise Control (CCC) (Ge and Orosz, 2014; Zhang and Orosz, 2016; Ge and Orosz, 2018) explored the benefits of the communication with remote preceding vehicle when the nearest preceding vehicle is unconnected, but a limitation was that CCC considered the behavior patterns of unconnected vehicles to be known (or identified) and unchanged given different drivers. These assumptions would be challenged in the real traffic situation.

A CACC extension considering Unconnected vehicle in the loop, dubbed as CACCu, was recently proposed in (Chen and Park, 2020). CACCu enables a vehicle to follow an unconnected vehicle with string stability, by utilizing the communication with a further connected preceding vehicle. Different from the existing CCC, CACCu aims to be robustly string-stable given various unconnected vehicles' car-following behaviors, without requiring identification process or extra information on the unconnected vehicles' behavior. Numerical simulations with real traffic data showed that the proposed CACCu can improve string stability, control accuracy and fuel efficiency compared to existing methods (Chen and Park, 2020).

To validate the effectiveness and feasibility of implementation, the CACCu system must be developed on actual vehicles and tested in the field. The sensor error and nonlinear vehicle dynamics have been shown the two major factors that could significantly deviate the actual performance of automated driving from that in the simulations. On one hand, the unexpected sensor noise in the real traffic may undermine the smoothness of vehicle response and force the designer to adopt more conservative control parameters. Taking dCACC (Ploeg et al., 2015) as example, the vehicle trajectories in the experiments with actual radar were much jerkier than those in simulations assuming radar distance/speed errors in normal distributions. Thus, a "slower" state estimation and longer desired headway should be applied for the ideal ride comfort. Similarly, although it is proved that ACC with Constant Time Gap (CTG) policy can guarantee string stability as the feedback gains are sufficiently high (Xiao and Gao, 2011), none of the commercial ACC systems (Milanes et al., 2014; Gunter et al., 2020) were string-stable as they were not able to use such high gains under the constraints of sensor noise and ride comfort. On the other hand, the nonlinear dynamics of real vehicles (especially those with internal-combustion engines) could prevent the vehicles from achieving the acceleration/speed as commanded. Previous tests (Ge et al., 2018; Nieuwenhuijze et al., 2012) have shown that the accuracy of vehicle longitudinal control can be heavily affected by the limited power of engine, the power drops during gear shifts, and other uncompensated nonlinear behaviors of the vehicle. In summary, field evaluation with physical vehicles is always a necessary step to verify that an automated driving application can achieve its benefits in the real world.

Additionally, it is noted that many previous demonstrations of CACC or related applications shared a drawback in the experiment setting. Their test scenarios were commonly constructed with fabricated traffic disturbance, instead of the real-world situations. For example, the leading vehicle of the CACC platoon followed a trapezoid speed profile in (Milanes et al., 2014), triangle speed profile in (Ploeg et al., 2011; Wei et al., 2018), and step speed profile in (Ploeg et al., 2015). The Grand Cooperative Driving Challenge (GCDC) adopted a speed profile which consisted of three swept sines with frequencies 0.01 rad/s–2 rad/s (van Nunen et al., 2012). While these test scenarios could conveniently examine the desired properties (e.g., string stability) of the tested control methods, they could not give quantitative insight on how much benefit the proposed methods could achieved over the existing ones (e.g., ACC) in the real life. To reasonably quantify the performance improvements, more realistic test scenarios should be utilized in the evaluations.

In this paper, the CACCu is tested with CAVs in real-world-based driving scenarios. While the original CACCu algorithm (Chen and Park, 2020) determines the optimal acceleration of the vehicle, the control algorithm is re-developed in this study based on the experiment vehicle which only accepts speed commands. Then, the effectiveness of CACCu, in comparison with ACC and human driving, is evaluated in the car-following scenarios constructed using the NGSIM (Alexiadis et al., 2004) real-traffic data. Because the test scenario of CACCu involves the unconnected preceding vehicle which is human-driven, another challenge is that the human always drives differently in the multiple runs (Ge et al., 2018). The inconsistent human behaviors may undermine the fairness of the

performance comparisons between different control methods. A more effective way, as shown later in this paper, is to replace the actual human-driven vehicle with an automated vehicle that is programmed to replay the recorded trajectory of an actual human-driven vehicle.

The rest of the paper is organized as follows: the second section introduces the automated vehicles used in the experiments. The third section describes the control design and parameterization of CACCu. The evaluation settings and the results are presented in fourth section. The key findings and concluding remarks are provided in the fifth section.

#### 2. Experimental vehicles

Two experimental vehicles, Hyundai i30 PD and Hyundai Veloster, are shown in Fig. 1. The i30 PD plays as the ego vehicle ruled by CACCu, while the Veloster is used to create the test scenarios, as explained later in the Section 4.1. Both vehicles have been equipped with onboard sensors and throttle/brake pedal actuators. The V2V communications between vehicle are enabled by Wi-Fi modules. The transmission rate of Wi-Fi message is set 10 Hz to mimic the well-known Basic Safety Massage (BSM) of Dedicated Short-Range Communication (DSRC), which may be implemented in the U.S. (Masini et al., 2018). Like BSM, the transmitted message contains time stamp, vehicle speed, acceleration, position (in X, Y, Z) and orientation (in X, Y, Z, W). However, CACCu only needs to use the vehicle acceleration, as stated in the next section

#### 2.1. Sensor selection

It is noted that the long-range radar sensor commonly adopted by commercial ACC systems is not available in these experimental vehicles. Instead, there are other two options for front-view sensing: Lidar (Velodyne 16ch Puck) and camera (Mobileye). To facilitate the selection of the appropriate sensor that meets the needs, a sensing accuracy experiment was conducted. The distance/speed relative to preceding vehicle, measured by Lidar and Mobileye during an arbitrary run are shown in Fig. 2. The real-time-kinetic (RTK) GPS, which is of centimeter accuracy, served as the ground truth. The results showed that the lidar sensor had a detection limit distance of 30 m. The reason is that the density of the point-cloud cluster gets too low as the distance increases. It was seen that the Mobileye estimated the depth of the preceding vehicle very well. The root mean square (RMS) values of the distance errors were found to be 1.10 m for Mobileye and 4.18 m for Lidar. Therefore, Mobileye was chosen to detect the preceding vehicle for CACCu. It is noted that Mobileye-based ACC has been deployed in some commercial vehicles (Mobileye, "Our Technology - Mobileye, 2021). The RMS error of estimated velocity by Mobileye was found to be 3.46 km/h (0.96 m/s), compared to the ground truth provided by CAN buses of ego and preceding vehicle. These are however notable sensing errors compared to state-of-art radar sensors (Hasch et al., 2012).

#### 2.2. Low-level controller and vehicle dynamics model

The experimental vehicles have been automated with a low-level controller (Jung et al., 2020), which regulates the throttle and brake pedals to achieve the speed command from a high-level controller (e.g., ACC or CACCu). This low-level controller has a cascade Proportional-Integral-Differential (PID) feedback form, consisting of a pedal control loop inside of the speed control loop. Details about the low-level controller can be found in (Jung et al., 2020). To be compatible with the existing low-level controllers, the original CACCu high-level controller which gives acceleration command (Chen and Park, 2020) must be redesigned, as described in the section Control Design.

With the low-level controller, a longitudinal vehicle dynamics model (VDM) of ego vehicle can be identified. In this case, the "vehicle dynamics" refers to the relationship between the commanded speed and the actual speed. A vehicle dynamics test was conducted for the model identification. Like in (Milanes et al., 2014); two small step signals (which caused no acceleration or braking saturation) were given as the commanded speed in the test, and the actual response of the vehicle was recorded. Using MATLAB system identification toolbox, a second-order model  $G_0(s)$  was identified from the collected data:



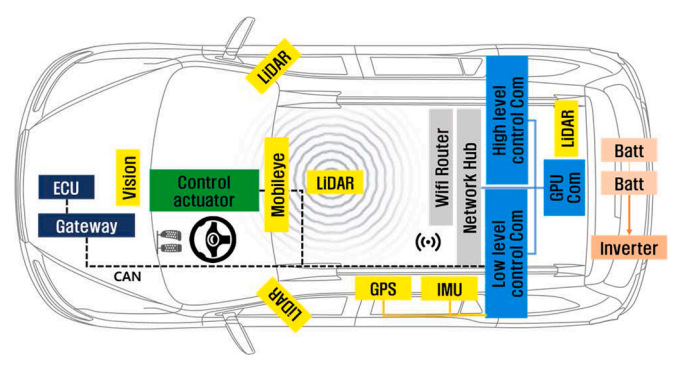


Fig. 1. Autonomous vehicle i30 PD (blue) / Veloster (yellow) and System Configure (right). (For interpretation of the references to colour in this figure legend, the reader is referred to the web version of this article.)

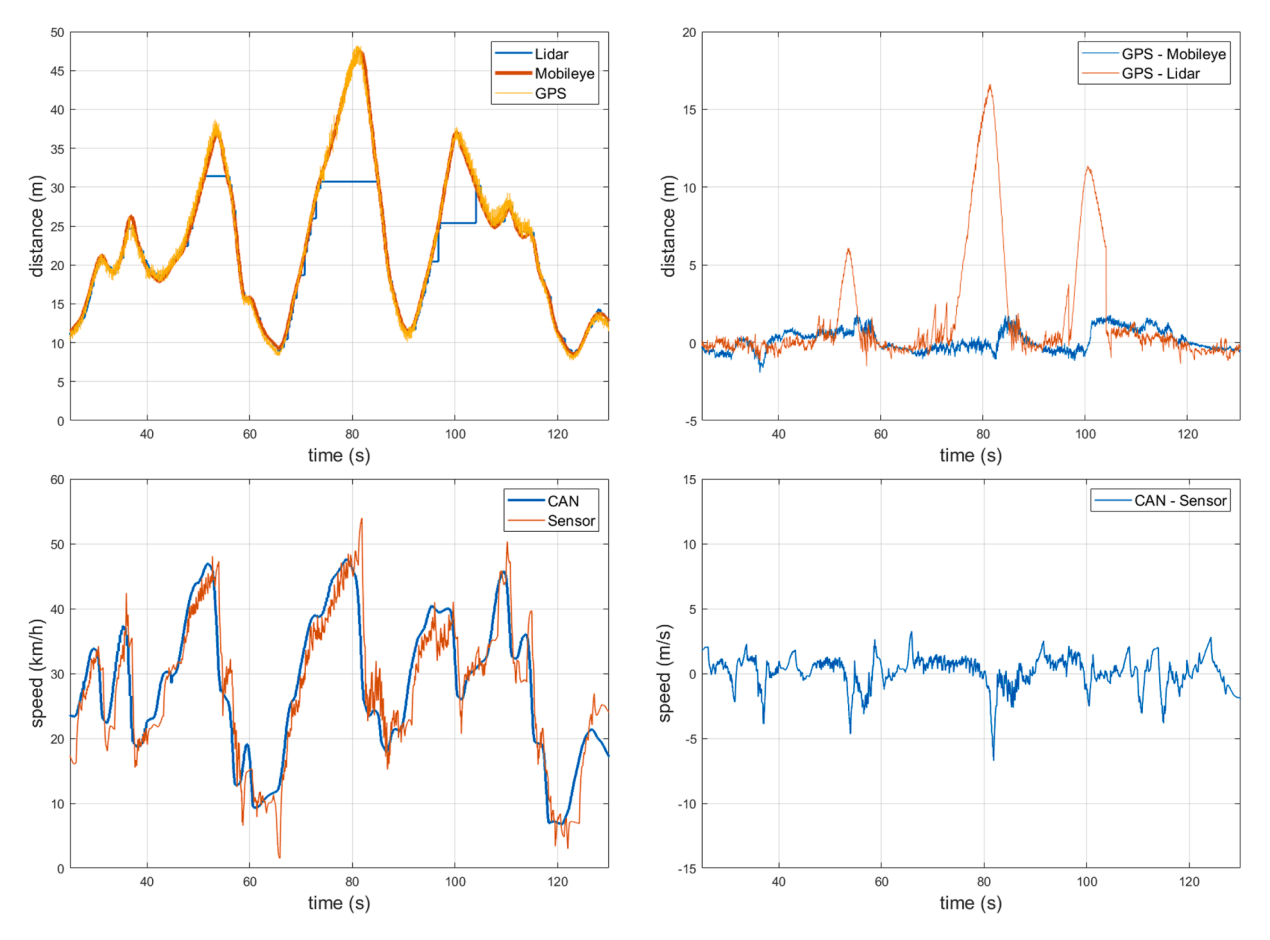


Fig. 2. Sensing results (left top/bottom) and sensing errors (right top/bottom).

$$G_0(s) = \frac{L(\dot{x}_0)}{L(v_c)} = \frac{1}{0.8s^2 + 1.6s + 1}e^{-0.5s}$$
 (1)

where  $\dot{x}_0$  and  $v_c$  are the speeds of ego vehicle and the commanded speed, respectively.  $L(^*)$  denotes Laplace transform and s is the Laplace variable. The commanded speed, the model response and the actual response of the vehicle are compared in Fig. 3. Considering the good match between the responses of model and vehicle, the identified model can reasonably represent the dynamics of the

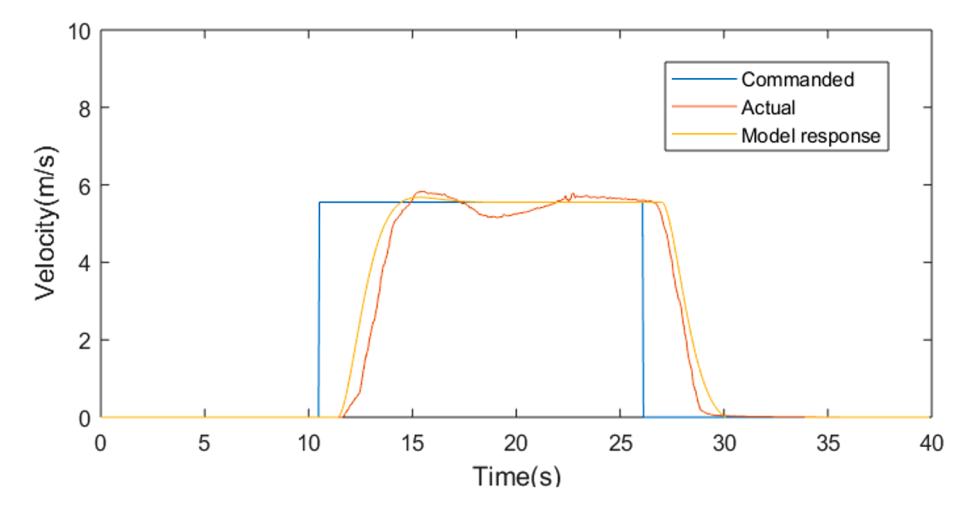


Fig. 3. The model response and actual vehicle response in the vehicle dynamics test.

experimental vehicle (Hyundai i30 PD).

#### 3. CACCu design

#### 3.1. Framework

It is a common strategy for a CACC vehicle to drive in ACC mode when encountering an unconnected preceding vehicle (Liu et al., 2018; Xiao et al., 2018). With CACCu, however, if there exists a further preceding vehicle which is connected, the ego vehicle may obtain additional benefits from the V2V communications, rather than completely falling back to ACC. For the ease of real-time implementation, this study pursues a linear time-invariant control design. Fig. 4 shows the feedback-feedforward control structure of the CACCu, which can be directly extended from an existing ACC or CACC system. The ACC controller generates a feedback control signal  $v_{fb}$  to regulate spacing error (i.e., the difference between desired distance and actual distance to the preceding vehicle), based on the sensor measurement and vehicle states. Meanwhile, a feedforward control signal  $u_{ff}$  can be generated to help prevent the spacing error that is about to occur, based on the communicated information from the further preceding vehicle, i.e., the  $(n+1)^{th}$  preceding vehicle. It is noted that the feedforward filter should be designed and tuned such that it can accommodate the uncertain behaviors of the n unconnected vehicles in between. The final control signal (i.e., the speed command) is the sum of  $v_{fb}$  and  $u_{ff}$ , and then a low-level controller determines the corresponding throttle or brake level to achieve the speed command.

#### 3.2. Human Car-following behavior

Since CACCu involves unconnected human-driven vehicle, it is important to incorporate the human car-following behavior. The physics-based optimal velocity model (OVM) (Ge and Orosz, 2017) is chosen to describe car-following behaviors of the unconnected vehicle around a traffic equilibrium:

$$h_1(t) = x_2(t) - x_1(t) - l$$

$$\ddot{x}_1(t) = \alpha_1(\frac{1}{t_{1,h}}h_1(t - \varphi_1) - \dot{x}_1(t - \varphi_1)) + \beta_1\dot{h}_1(t - \varphi_1)$$
(2)

where t is time,  $\dot{*}/\ddot{*}$  denotes the variable's first/second derivative in respect to time,  $x_1(t)$  and  $x_2(t)$  are locations of the human-driven vehicle and its preceding vehicle,  $h_1$  is the adjustable gap between the two vehicles, with l being the minimum bumper-to-bumper distance,  $\alpha_1$  and  $\beta_1$  are human control gains,  $\varphi_1$  is the human delay (i.e., reaction time),  $\frac{1}{t_{1,h}}$  is spacing policy slope with  $t_{1,h}$  being the desired time gap of the human driver. In fact, other frequently used car-following models (e.g., intelligent driver model) can be linearized into the same form of this OVM (Ge and Orosz, 2017).

Taking Laplace transform of (2), the human-driven vehicle's behavior can be represented by a transfer function in Laplace domain:

$$T_1(s) = \frac{L(x_1(t))}{L(x_2(t))} = \frac{K_1(s)}{s^2 e^{\varphi_1 s} + K_1(s) + \alpha_1 s}$$
(3)

where L(\*) denotes Laplace transform, s is the Laplace variable and  $K_1(s) = \frac{a_1}{t_{1,h}} + \beta_1 s$ .

Due to the heterogeneity of human drivers in the real traffic, this study considers human parameters in normal distributions based on previous investigations (Ayres et al., 2001; Mehmood and Easa, 2009; Ge and Orosz, 2017):

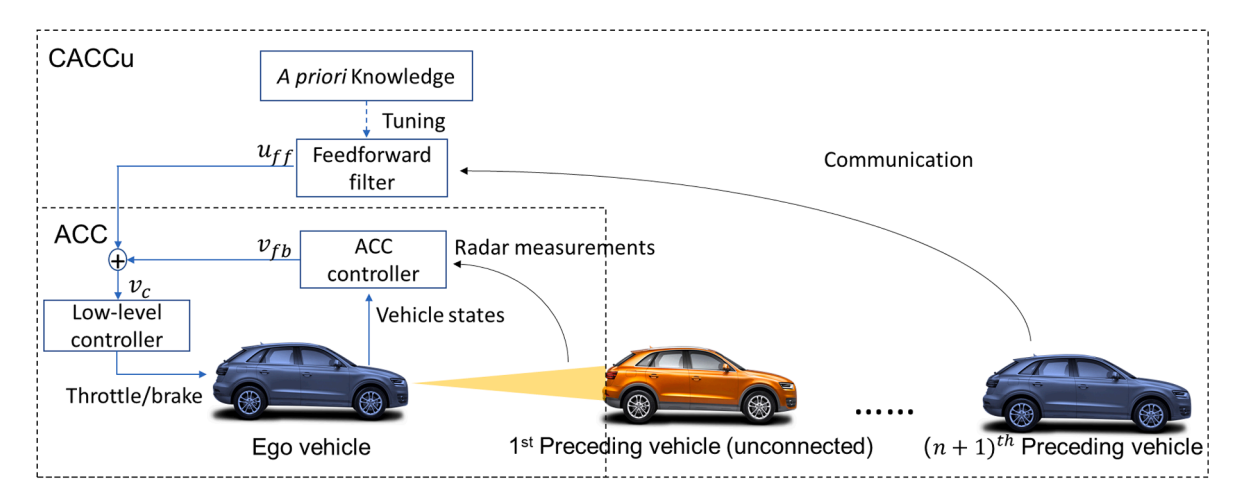


Fig. 4. Framework of CACCu.

- Desired headway  $t_{1h} \sim N(1.5, 0.25^2)$ ;
- Human delay  $\varphi_1 \sim N(1, 0.25^2)$ ;
- Human gain  $\alpha_1 \sim N\left(0.2, \left(\frac{0.2}{2.6}\right)^2\right)$ ;
- Human gain  $\beta_1 \sim N\left(0.4, \left(\frac{0.4}{2.6}\right)^2\right)$

These distributions are to be used to parameterize a CACCu controller that is robust against the variety of human car-following behaviors.

#### 3.3. Control design

The general goal of ACC or CACCu is to maintain a desired spacing in respect to the immediately preceding vehicle. The widely-accepted Constant-Time-Gap (CTG) spacing policy (Naus et al., 2010) is adopted in this study, and the corresponding desired spacing of ego vehicle reads:

$$h_{0,d}(t) = t_{0,h}\dot{x}_0(t) + h_{0,st}$$
 (4)

where  $h_{0,d}(t)$  is the desired spacing,  $h_{0,st}$  is the standstill spacing,  $t_{0,d}$  is the desired time gap, and  $\dot{x}_0(t)$  is the speed of ego vehicle.

#### ACC controller:

In ACC, the onboard sensor can measure the actual spacing and relative speed in respect to the 1st preceding vehicle:

$$h_0(t) = x_1(t) - x_0(t) - l_1$$
 (5)

where  $h_0$  is the actual inter-vehicle spacing,  $x_0(t)$  and  $x_1(t)$  are the locations of the ego and 1st preceding vehicle, with  $l_1$  being the length of the 1st preceding vehicle.

The controller should be able to eliminate the spacing error, i.e., the difference between the actual spacing and the desired spacing  $h_{0,d}$ . The spacing error and spacing error rate can be determined as below:

$$e_0(t) = h_0(t) - h_{0,d}(t) = x_1(t) - x_0(t) - t_{0,h}\dot{x}_0(t) - h_{0,st} - l_1$$

$$(6)$$

$$\dot{e}_0(t) = \dot{h}_0(t) - t_{0,h}\ddot{x}_0(t)$$
 (7)

 $e_0(t)$  is the spacing error;  $\dot{e}_0(t)$  is the spacing error rate,  $\dot{h}_0(t)$  is the relative speed measured by the onboard sensor, and  $\ddot{x}_0(t)$  is the ego vehicle's acceleration obtained from its CAN bus.

Then a Proportional-Derivative (PD) controller is used to generate the feedback control signal:

$$v_{fb}(t) = \dot{x}_0(t) + k_p e_0(t) + k_d \dot{e}_0(t) \tag{8}$$

where  $v_{fb}(t)$  is the feedback control signal, and  $k_p$  and  $k_d$  are the gains of the PD controller. Note that (8) can stand alone as an ACC controller, where  $v_{fb}(t)$  is directly given to the low-level controller as the ACC speed command. The control scheme of ACC is displayed in Fig. 5, where  $G_0(s)$  is as defined in (1) and

$$K_0(s) = k_p + k_d s$$

$$H_0(s) = 1 + t_h s$$

Accordingly, the car-following behavior of the ACC vehicle can be represented by a transfer function:

$$T_0(s) = \frac{X_0(s)}{X_1(s)} = \frac{G_0(s)K_0(s)H_0(s)}{H_0(s)(s + G_0(s)H_0(s)K_0(s) - G_0(s)s)}$$
(9)

where

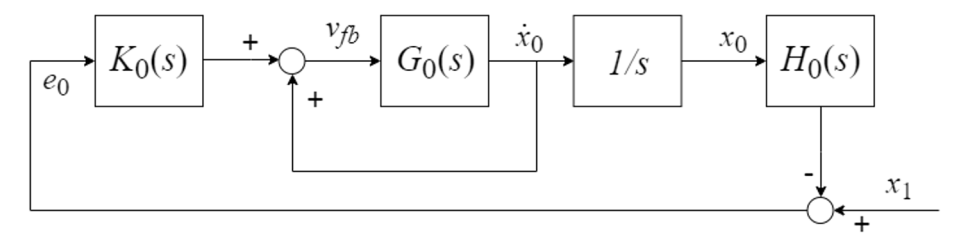


Fig. 5. Control scheme of ACC.

$$X_0(s) = L(x_0(t))$$

$$X_1(s) = L(x_1(t))$$

To fulfill the internal stability (Doyle et al., 2013) of the ego vehicle, the poles (i.e., zeros of its denominator) of (9) should have negative real parts. This study adopts a desired time gap  $t_h = 1.5s$ , a common option in commercial ACC systems (Gunter et al., 2020). Then the control gains  $k_0$  and  $k_d$  are left to be tuned.

Besides the internal stability, the tuned gains should guarantee the basic smoothness and accuracy of control, under the sensor errors and the imperfect vehicle dynamics. Based on the experience of previous ACC designs (Naus et al., 2010; Ploeg et al., 2015; Nieuwenhuijze et al., 2012), the  $k_d$  is commonly larger than  $k_p$  to achieve reasonable vehicle behaviors. For the safety and convenience, the gain tuning was conducted using numerical simulations in MATLAB-Simulink. The designed ACC system was modeled and simulated in a typical car-following scenario used in (Chen and Park, 2020). The sensor errors observed in Section 2.1 were modeled as normal random noise, and the vehicle dynamics model followed (1). The speed profiles of the ACC with some different gains are shown in Fig. 6.

Eventually, the gains were determined to be  $(k_p, k_d) = (0.5, 1)$  which fulfill the internal stability, and showed a good balance between control accuracy and smoothness.

#### CACCu controller:

In CACCu mode, the ego vehicle can be aided by an extra feedforward signal:

$$v_c(t) = v_{fb}(t) + u_{ff}(\ddot{x}_{n+1}(t-\theta))$$
 (10)

where  $v_c(t)$  is the speed command,  $u_{ff}(t,\ddot{x}_n)$  is the feedforward signal,  $\ddot{x}_n$  is the acceleration of the  $(n+1)^{th}$  preceding vehicle, and  $\theta$  is the communication delay. While CACCu can be extended for more general scenarios (Chen and Park, 2020), this demonstration focuses on three-vehicle sandwich scenario (i.e., one unconnected vehicle is in between the two connected vehicles), which has the highest probability to occur in the mixed traffic (Chen and Park, 2020). Thus, we denoted n=1 in the rest of paper. The control scheme of CACCu is shown in Fig. 7, where F(s) is the feedforward filter in Laplace domain and  $D(s) = e^{-\theta s}$ .

To determine a feedforward filter that generates proper  $u_{ff}$ , we combine (1) and the Laplace transforms of (4)–(7) and (10), yielding:

$$L(e_0(t)) = X_1(s) - H_0(s)X_0(s) = X_1(s) - \frac{H_0(s)G_0(s)X_0(s)X_1(s) + H_0(s)G_0(s)F(s)s^2X_2(s)}{s + G_0(s)H_0(s)X_0(s) - G_0(s)s}$$

$$(11)$$

By making  $L(e_0(t)) = 0$ , the ideal feedforward filter F(s) can be derived to eliminate the spacing error:

$$F(s) = \frac{1 - G_0(s)}{sH_0(s)G_0(s)D(s)} \frac{X_1(s)}{X_2(s)} = \frac{1 - G_0(s)}{sH_0(s)G_0(s)D(s)} T_1(s)$$
(12)

where  $T_1$  is the transfer function of unconnected preceding vehicle, as defined in (3). Because the human parameters in  $T_1$  and the communication delay D(s) cannot be exactly known, a more feasible feedforward filter is:

$$F(s) = \frac{1 - G_0(s)}{sH_0(s)G_0(s)}T_1(s) \tag{13}$$

where  $T_1(s)$  is the transfer function of a "virtual preceding vehicle", in the same form of  $T_1(s)$ :

$$T_1(s) = T_1(\alpha_1, \beta_1, \varphi_1, t_{1,h}, s)$$
 (14)

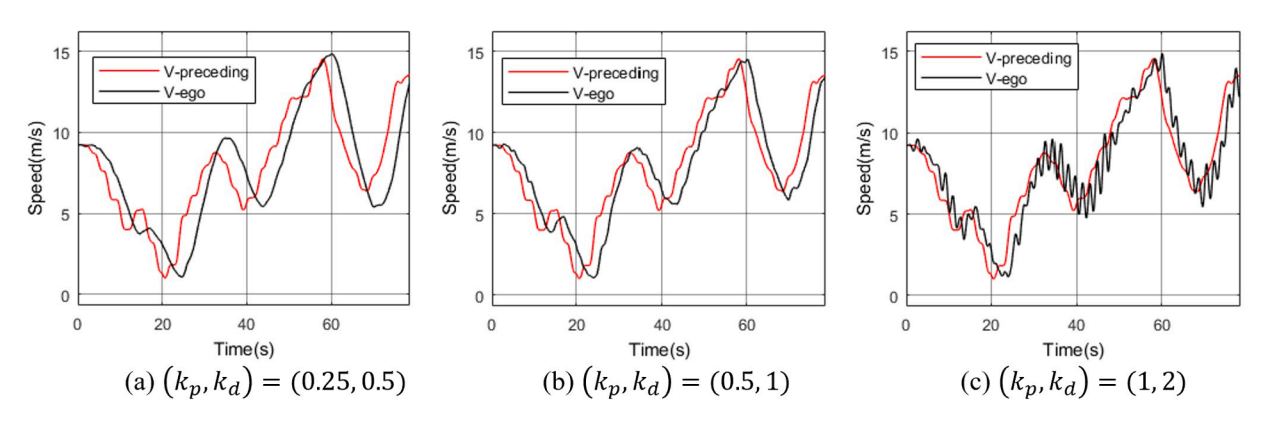


Fig. 6. Speed profiles of the simulated ACC vehicle with different gains in a typical car-following scenario.

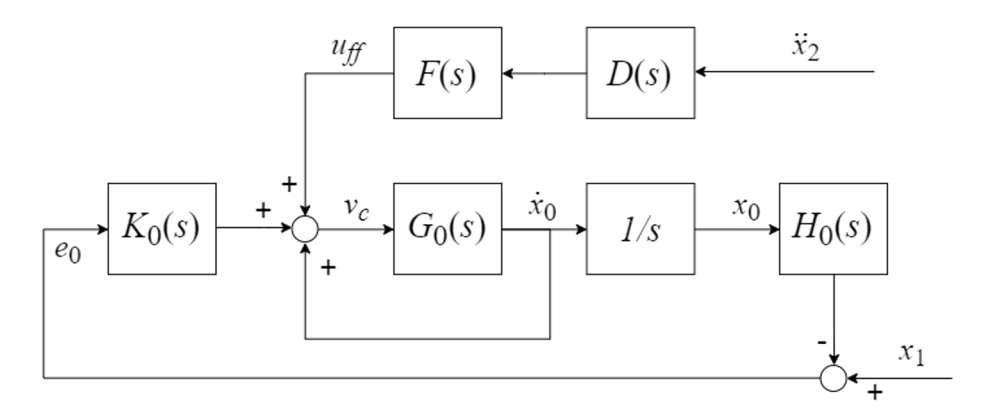


Fig. 7. Control scheme of CACCu.

 $\vec{\alpha_1}, \vec{\beta_1}, \vec{\varphi_1}, \vec{t_{1,h}}$  are the parameters of the virtual preceding vehicle.

Combining (3), (11) and (13), the car-following behaviors of CACCu vehicle can be expressed as:

$$T_0(s) = \frac{X_0(s)}{X_1(s)} = \frac{G_0(s)K_0(s)H_0(s) + D(s)(s - G_0(s)s)T_1(s)/T_1(s)}{H_0(s)(s + G_0(s)H_0(s)K_0(s) - G_0(s)s)}$$
(15)

Since (15) has the same denominator with (9), the internal stability of ego vehicle in CACCu mode is fulfilled given the same feedback control parameters. However, we need to further determine  $T_1(s)$  in pursuit of the string stability.

#### 3.4. Parameterization for string stability

While there exist multiple mathematical definitions of string stability, a widely-used and convenient one is defined in frequency domain (van Nunen et al., 2012), that is, the frequency response magnitude of  $T_0(s)$  should always be no greater than 1:

$$||T_0(j\omega)||_{\infty} \le 1 \tag{16}$$

where  $\|\cdot\|_{\infty}$  denotes the maximum magnitude over all frequency  $\omega \geq 0$ , and j is the imaginary unit. Because  $T_0(j\omega) = \frac{L(x_0(t))}{L(x_1(t))} = \frac{L(x_0(t))}{L(x_1(t))}$ 

 $\frac{L\left(\dot{x_0}(t)\right)}{L\left(\dot{x_1}(t)\right)} = \frac{L\left(\dot{x_0}(t)\right)}{L\left(\ddot{x_1}(t)\right)}$ , condition (16) can be approximately interpreted as that given any perturbation from the downstream, the speed or

acceleration peak of following vehicle should not exceed that of the preceding vehicle. Although string stability can also be tested in terms of spacing error or control input (Naus et al., 2010), they are less practical as the human driver is involved.

For ACC, it can be found that  $T_0(s)$  defined by (9) does not satisfy (16) unless the desired time gap is significantly raised to 2.9 s. For CACCu,  $T_0(s)$  in (15) collapses to  $1/H_0$  and automatically satisfy (14) if there is no communication delay (D=1) and  $T_1=T_1$ . However, there is rare chance to make  $T_1=T_1$  in the implementation. Instead, we parameterize  $T_1$  to achieve the string stability for the highest probability given various  $T_1$ . Accordingly, String Stability Ratio (SSR) is defined as the probability that CACCu vehicle can stay string-stable given all different kinds of unconnected preceding vehicles. By definition, SSR can be computed as an integral of the probability density over all the string-stable combinations of  $(\alpha_1, \beta_1, \varphi_1, t_{1,h})$ :

$$SSR = \int \int \int \int p(\alpha_1, \beta_1, \varphi_1, t_{1,h}) \xi(SS) d\alpha_1 d\beta_1 d\varphi_1 dt_{1,h}$$
(17)

where p is the probability density function (PDF) of a combination of human parameters  $(a_1, \beta_1, \varphi_1, t_{1,h})$  which can be calculated according to the aforementioned distributions of the human parameters, and

$$\xi(\mathit{SS}) = \left\{ \begin{matrix} 1 & \mathit{if} \;\; \mathit{SS} \leq 1 \\ 0 & \mathit{if} \;\; \mathit{SS} > 1 \end{matrix} \right.$$

Then the optimal virtual preceding vehicle  $T_1$  can be found by maximizing SSR. Using MATLAB nonlinear optimization toolbox,  $\alpha_1$ ,  $\beta_1$ ,  $\varphi_1$ ,  $t_{1,h}$  are determined to be (1.12, 0.21, 0, 1.62) which leads to a maximum SSR = 95%.

Fig. 8 provides an insight on the broad ranges of the preceding vehicle's human parameters that the current CACCu can stay string-stable with. Fig. 8 (a) shows string-stable ranges (the blanked area) of  $\alpha_1$  and  $\beta_1$  (fixing  $\varphi_1 = 1, t_{1,h} = 1.5$ ), while Fig. 8 (b) shows string-stable ranges of  $\varphi_1$  and  $t_{1,h}$  (fixing  $\alpha_1 = 0.2, \beta_1 = 0.4$ ). It can be seen that CACCu can fulfill string stability under most of human behaviors of the unconnected preceding vehicle.

#### 4. Performance evaluation

#### 4.1. Experiment settings

In the evaluation of CACCu, ACC and human driving serve as performance baselines. It is noted that an actual human driver, instead of any driver model or trajectory data was employed to perform the "human driving" in the field experiment.

To ensure fair comparisons among CACCu, ACC and human driving, it is required that two preceding vehicles must drive identically each time when testing different control methods. However, a difficulty is that the 1st preceding vehicle is supposed to be a human-driven vehicle while it is almost impossible for the human driver to follow the test path the same way as before. Therefore, we proposed to use the existing NGSIM data (Alexiadis et al., 2004), collected by Federal Highway Administration (FHWA) in real roads, to reconstruct the real-traffic scenarios. In every test scenario, the NGSIM trajectories of two consecutive vehicles (i.e., 1st and 2nd preceding vehicles) are extracted. As shown in Fig. 9, the Hyundai Veloster is set in automated mode instead of manual model. The speed profile of 1st preceding vehicle from NGSIM is given to the Veloster as speed command over time, so that the movement of 1st preceding vehicle can be replicated consistently.

As the ego vehicle does not need to sense the 2nd preceding vehicle and the trajectories of both preceding vehicles are fixed, there is no need to physically add a 2nd preceding vehicle to the test. An easier but equivalent way is making the Hyundai Veloster imitate the communications from the 2nd preceding vehicle to ego vehicle. Then, the Hyundai i30 (ego vehicle) can be driven in CACCu/ACC/human mode following the Veloster.

Three test scenarios are randomly extracted from the NGSIM data. The speed profiles of the 1st and 2nd preceding vehicles in these scenarios are shown in Fig. 10. Note that a moderate acceleration period of  $0.5m/s^2$  has been added to the beginning of each NGSIM vehicle speed profile so that the test vehicles can gently reach the starting-point speed from the rest. The performance of ego vehicle during this start-up period are not taken into the results. This study set the standstill spacing in (4) as 15 m for securing the safety, while shorter one could be used in the implementation to increase road throughput. To disperse the random effects of vehicle dynamics non-linearity and sensor errors, each control method was tested twice in every scenario.

This experiment was conducted at a 1 km straight track administrated by the Korea Advanced Institute of Science and Technology (KAIST). Fig. 11 shows the two experimental vehicles on the test track. There was no precipitation during the experiment and the road was mostly dry.

#### 4.2. Results

The Root Mean Squares (RMS) of acceleration and spacing error of the ego vehicle were collected, as performance measures in comfort and control accuracy, respectively.

Because the fuel consumption in each run was not obtainable, the popular VT-CPFM (Rakha et al., 2011) model was used to estimate a nominal fuel consumption based on the ego vehicle's trajectory. The model reads:

$$FC(t) = \begin{cases} a_0 + a_1 P(t) + a_2 P(t)^2, & P(t) \ge 0\\ a_0, & P(t) < 0 \end{cases}$$
 (18)

where FC(t) is the consumed fuel at the instant t;  $a_0$ ,  $a_1$  and  $a_2$  are model constants calibrated for each vehicle; P(t) is the power exerted by the vehicle driveline at instant t, a function of the vehicle speed and acceleration. The value of  $a_0$ ,  $a_1$ ,  $a_2$  and coefficients in P(t) should be determined based on vehicle-specific parameters (mass, air-drag coefficient, cylinder size, etc.). More details about the

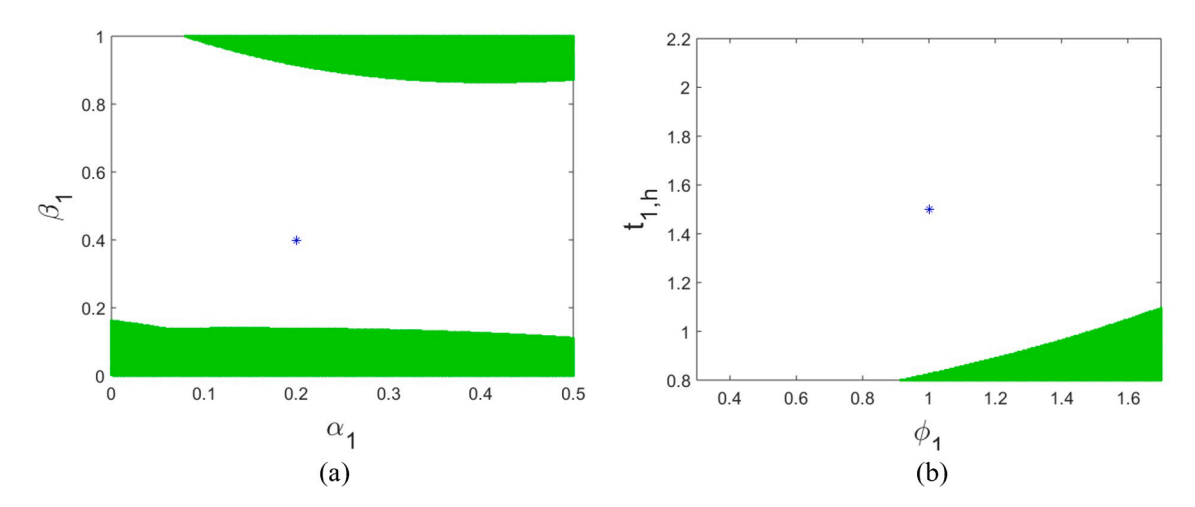


Fig. 8. String-stable ranges of the preceding vehicle's human parameters.

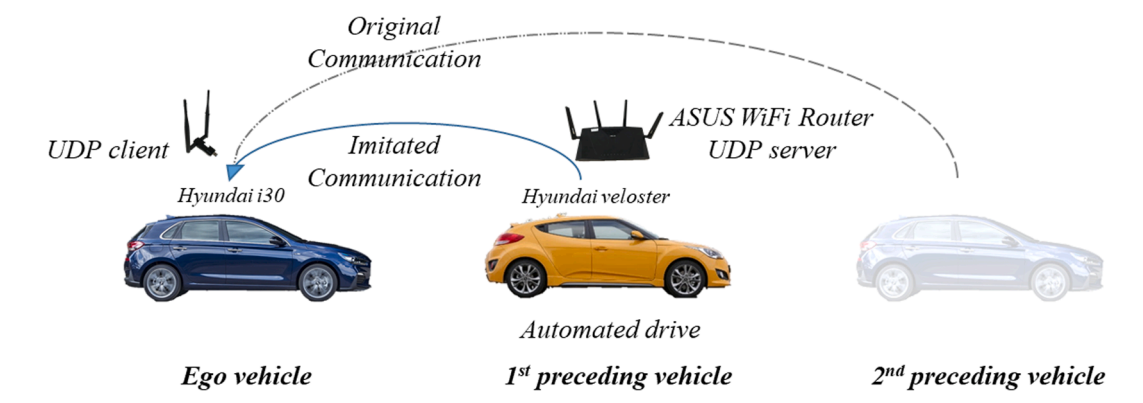


Fig. 9. Re-producing the three-vehicle-sandwich scenario.

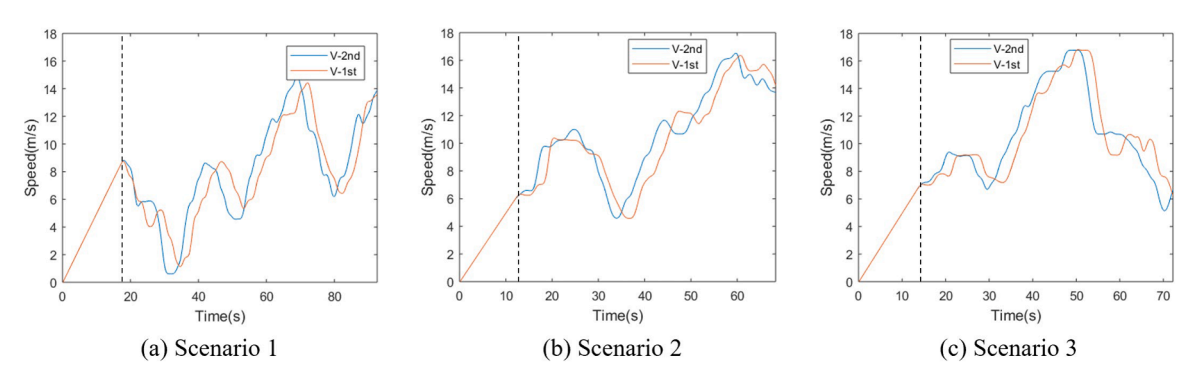


Fig. 10. The speed profiles of the preceding vehicles in test scenarios.



Fig. 11. Experimental vehicles on the test track.

required vehicle parameters and model calibration process can be found in (Rakha et al., 2011).

The VT-CPFM was validated through field tests of typical light-duty vehicles (Rakha et al., 2011) and has been applied in many related works (Zohdy et al., 2012; Yang et al., 2017). It should be noted that the interest of this study is the relative differences among the control methods, not the absolute value of the fuel consumption. Therefore, the VT-CPFM is useful in this study even though it was calibrated using other vehicles.

The test results of CACCu/ACC/human driving are summarized in Table 1. CACCu consistently outperformed ACC and human driver in all aspects:

- Compared with ACC, CACCu in average reduced 10.8% acceleration RMS, 60.8% spacing error RMS and 6.2% fuel consumption. CACCu maintained the desired time gap more precisely and with even less control effort than the ACC did. These results corroborate the benefits of CACCu shown in the simulation study (Chen and Park, 2020).
- Compared with human driving, CACCu reduced 17.6% acceleration and 13.3% fuel consumption, indicating great advantages in
  ride comfort and energy efficiency. The spacing error was not applicable to human driving as the human driver's desired spacing is
  unknowable.

Another important design goal of CACCu is to achieve string stability, i.e., the capability of attenuating the traffic disturbance. The vehicle speed profiles of CACCu/ACC/human driving in tests 1.1, 2.1 and 3.1 are displayed in Fig. 12. The speed overshootings, indicators of amplified traffic disturbance, are denoted by the red arrows. It can be seen that CACCu tended to mitigate the speed fluctuations from the downstream vehicles in most of time. Across the total 6 tests, CACCu had only one speed overshooting in the test 3.1, as shown in Fig. 12 (g). By contrast, ACC and human driving frequently produced speed overshootings in every test, which explained for the higher acceleration and fuel consumption than CACCu's. Fig. 13 further shows the spacing profiles of ego vehicle under CACCu, ACC and human driving. CACCu had the least magnitudes of the spacing fluctuations in all the test scenarios. The numerical measures regarding traffic disturbance are listed in Table 2. In average, CACCu reduced 88.9% speed overshootings, 6.53% speed Standard Deviation (STD), and 26.39% spacing STD from those of ACC. These benefits remain similar when comparing CACCu with human driving. According to the results above, the string stability of CACCu is significantly better than that of ACC or human driving.

In addition, it is noted that the 1st preceding vehicle produced almost identical speed profiles in the same test scenario but different runs of CACCu, ACC and human driving. Thus, the experiment setting for the fair comparison between control methods is proven effective.

#### 4.3. Extensive evaluation

Due to the high cost of preparing and running the field test, the performance of CACCu could only be tested in a limited number of scenarios. To extensively reveal the benefits of CACCu in more various scenarios, numerical simulations were conducted using a full NGSIM dataset collected from US highway101 (US101). The US101 dataset was collected by FWWA to reflected the high-density highway traffic conditions. We in total extracted 380 car-following scenarios lasting longer than 50 s, from this US101 dataset. The main simulation settings are as below:

- The sensor errors identified in Section 2.1 are modeled as normal random noise;
- The vehicle dynamics model follows (1) in the simulations. Besides (1), the vehicle' maximum acceleration is set to be 5  $m/s^2$ , based on historical test data;

**Table 1**Performances measures under CACCu/ACC/Human driving.

Test number	Control type	Acceleration RMS(m/s)	Spacing error RMS(m)	Fuel consumption (ml)
1.1	CACCu	0.72	1.86	41.80
	ACC	0.85	3.48	42.80
	Human	0.84	N/A	45.50
1.2	CACCu	0.77	1.95	41.70
	ACC	0.87	5.44	41.60
	Human	0.95	N/A	48.90
2.1	CACCu	0.70	2.03	43.10
	ACC	0.75	5.42	43.60
	Human	0.77	N/A	46.80
2.2	CACCu	0.74	1.97	42.50
	ACC	0.74	5.24	44.20
	Human	0.90	N/A	48.40
3.1	CACCu	0.61	1.97	37.30
	ACC	0.86	5.60	48.20
	Human	0.85	N/A	46.20
3.2	CACCu	0.81	2.33	43.00
	ACC	0.80	5.70	45.60
	Human	0.97	N/A	52.30
Average	CACCu	0.72	2.02	41.57
	ACC	0.81	5.15	44.33
	Human	0.88	N/A	48.02
Reduction	From ACC (%)	10.82%	60.79%	6.24%
	From Human (%)	17.64%	N/A	13.43%

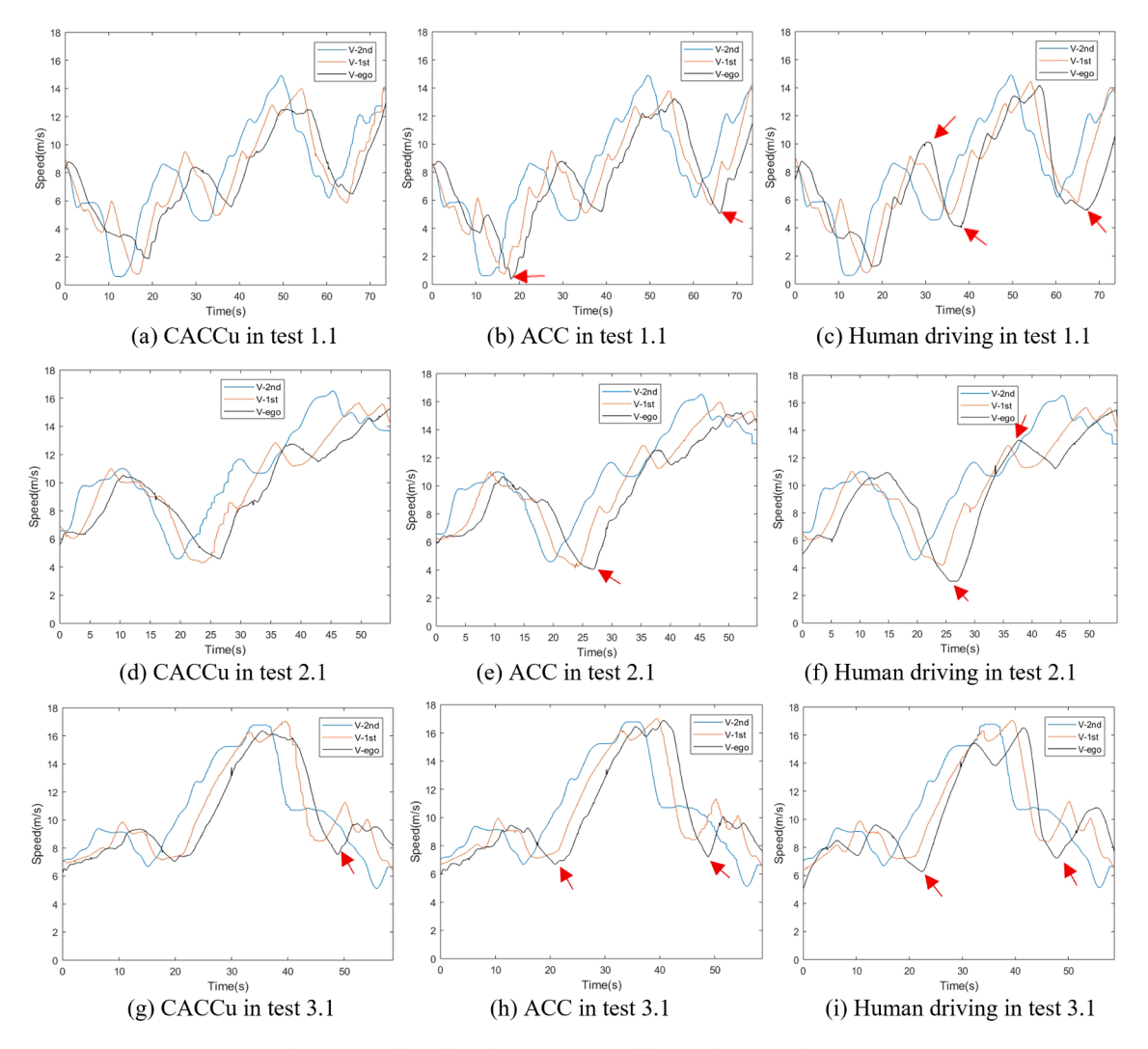


Fig. 12. Speed profiles of CACCu, ACC and human driving in the tests.

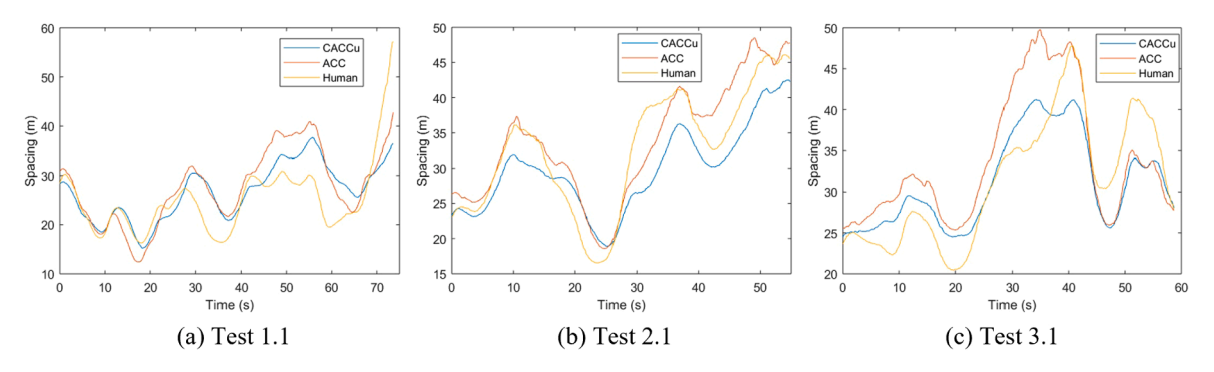


Fig. 13. Spacing profiles of CACCu, ACC and human driving in the tests.

• The communication delay is assumed to be 0.1 s, which is the most observed value in field tests.

Before going forward, the simulations were conducted using a field-test scenario to verify the fidelity. The speed profiles of actual and simulated CACCu/ACC vehicle in test 1.1 are compared in Fig. 14. It can be seen that the simulated speed of ego vehicle stays close to the actual speed in most of time, which indicates a good fidelity of the simulation.

**Table 2**Measures of traffic disturbance under CACCu/ACC/Human driving.

Test number	Control type	Count of speed overshootings	Speed STD	Speed range	Spacing STD	Spacing range
1.1	CACCu	0	2.94	11.11	5.53	22.44
	ACC	2	3.12	12.87	7.37	30.31
	Human	1	3.25	12.44	5.70	27.76
1.2	CACCu	0	3.05	11.52	5.69	24.06
	ACC	2	3.12	13.14	7.92	29.31
	Human	3	3.34	12.91	6.32	37.05
2.1	CACCu	0	2.92	10.65	5.89	23.56
	ACC	0	3.22	11.44	8.12	29.94
	Human	2	3.64	12.45	6.56	24.03
2.2	CACCu	0	2.95	10.34	5.82	22.19
	ACC	1	3.21	11.20	8.09	29.94
	Human	2	3.45	12.47	8.30	29.56
3.1	CACCu	1	3.09	10.13	5.56	16.75
	ACC	2	3.26	10.93	7.68	24.44
	Human	2	3.29	11.34	5.29	18.38
3.2	CACCu	0	2.97	9.87	6.07	20.44
	ACC	2	3.24	10.72	7.77	24.31
	Human	3	3.06	11.45	7.44	27.38
Average	CACCu	0.17	2.99	10.60	5.76	21.57
	ACC	1.50	3.20	11.72	7.82	28.04
	Human	2.17	3.34	12.18	6.60	27.36
Reduction	From ACC (%)	88.89%	6.53%	9.48%	26.39%	23.07%
	From Human(%)	92.31%	4.23%	12.91%	12.74%	21.16%

Then, the simulations of CACCu/ACC in the extensive 380 scenarios were conducted and the average performance measures are reported in Table 3. It is noted that the performance of "human" here is calculated from trajectories of the actual ego vehicle (i.e., the actual vehicle behind the 1st preceding vehicle) stored in the US101 dataset. In average, CACCu reduced 4.7% acceleration RMS, 60.8% spacing error RMS and 6.2% fuel consumption from ACC's. The reductions in acceleration and fuel consumption are even greater when compared with human driving. Paired T-test indicates all the benefits of CACCu are statistically significant (p < 0.05).

These simulation results in various scenarios confirm the finding in the field test, i.e., the CACCu can maintain the desired time gap much more precisely with even less control effort, compared with ACC.

#### 5. Conclusions and future work

CACC with Unconnected vehicle in the loop (CACCu) is a potential application to extend the usability of cooperative longitudinal control of Connected Automated Vehicles (CAVs) in the mixed traffic. To validate the feasibility of CACCu for future implementation, this study developed a CACCu system based on real vehicles and evaluate it in the field. A speed-command-based CACCu algorithm is designed according to the identified longitudinal dynamics of the experimental vehicle. The controller is parameterized by optimizing the String Stability Ratio (SSR), which indicates the likelihood to make the ego vehicle string-stable given various driving habits of the unconnected preceding vehicles.

The experiment was conducted with two automated vehicles equipped with Mobileye sensors and Wi-Fi modules. By commanding the 1st preceding to follow a NGSIM real-traffic trajectory, and simultaneously spread the information of the 2nd preceding vehicle in

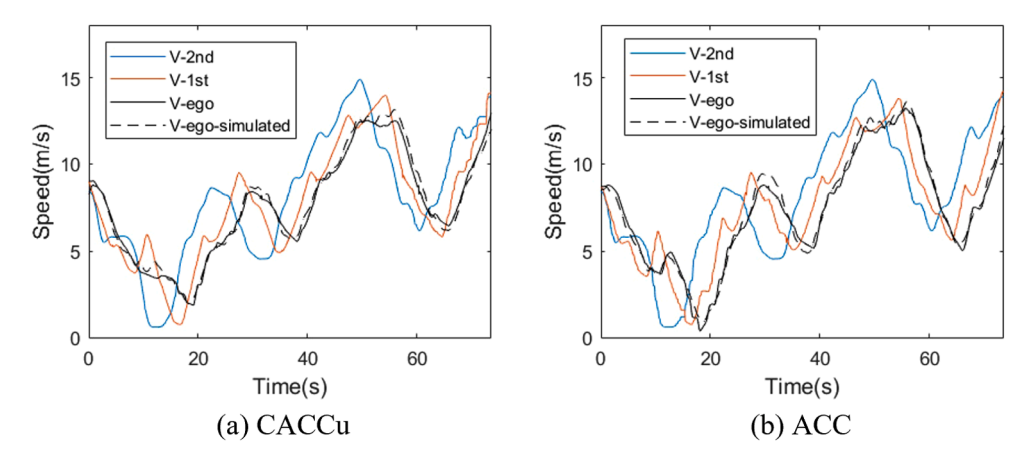


Fig. 14. Speed profiles of actual and simulated CACCu/ACC vehicle in test 1.1.

**Table 3**Average performances of CACCu/ACC/human in the 380 simulated scenarios.

	Control type	Acceleration RMS(m/s)	Spacing error RMS(m)	Fuel consumption (ml)
Average	CACCu	0.73	1.53	43.81
	ACC	0.77	2.70	45.77
	Human (NGSIM)	0.89	N/A	47.58
Reduction	From ACC (%)	4.7%	43.4%	4.3%
	From Human(%)	18.1%	N/A	7.9%

NGSIM data, CACCu was able to be tested in three-vehicle-sandwich scenarios with only two actual vehicles. ACC and human driving served as performance baseline in the evaluation. Over the 6 test runs for each control method, it was found that CACCu reduced 10.8% acceleration RMS, 60.8% spacing error RMS and 6.2% fuel consumption from ACC's. Compared with human driving, CACCu reduced 17.6% acceleration and 13.4% fuel consumption. The speed profiles of vehicles showed that CACCu greatly attenuated the traffic disturbances while ACC and human driving tended to amplify them. Therefore, the experiment results show that CACCu can greatly attenuate the traffic disturbance and improve the car-following control accuracy, ride comfort, and fuel efficiency. To extensively reveal the benefits of CACCu in more various scenarios, numerical simulations were conducted using the 380 car-following scenarios collected in US highway101 (US101), which confirmed the benefits of CACCu.

Future work includes the experiments of CACCu in more generalized traffic situations (e.g., multiple unconnected vehicles in between) rather than three-vehicle-sandwich scenarios emphasized by this study. Hardware-in-the-loop simulation could be utilized to rapidly and safely test CACCu in complicated scenarios. Besides, sophisticated control frameworks such as Adaptive Model Predictive Control (A-MPC) (Fukushima et al., 2007) can be adopted for handling the uncertain human behaviors more efficiently and further improving the performance of CACCu, although more computational resource may be required in such case. Lastly, the coordination between the CACCu vehicles and traffic signal is worth study for benefiting the mixed traffic in urban corridors.

#### CRediT authorship contribution statement

**Daegyu Lee:** Validation, Data analysis, Writing - original draft, Writing - review & editing. **Seungwook Lee:** Validation, Data analysis, Writing - original draft, Writing - review & editing. **Zheng Chen:** Conceptualization, Methodology, Data analysis, Writing - original draft, Writing - review & editing. **B. Brian Park:** Conceptualization, Methodology, Supervision, Writing - original draft, Writing - review & editing. **David Hyunchul Shim:** Writing - original draft, Writing - review & editing.

#### **Declaration of Competing Interest**

The authors declare that they have no known competing financial interests or personal relationships that could have appeared to influence the work reported in this paper.

#### Acknowledgement

This research is in part supported by the National Science Foundation under Grant No. CMMI-2009342.

#### References

Alexiadis, V., Colyar, J., Halkias, J., Hranac, R., McHale, G., 2004. The next generation simulation program. ITE J. (Institute Transp. Eng.) 74 (8), 22-26.

Ayres, T.J., Li, L., Schleuning, D., Young, D., 2001. Preferred time-headway of highway drivers. In: ITSC 2001. 2001 IEEE Intelligent Transportation Systems. Proceedings (Cat. No.01TH8585), 2001, pp. 826–829, doi: 10.1109/ITSC.2001.948767.

Bansal, P., Kockelman, K.M., 2017. Forecasting Americans' long-term adoption of connected and autonomous vehicle technologies. Transp. Res. Part A Policy Pract. 95, 49–63. https://doi.org/10.1016/j.tra.2016.10.013.

Chen, Z., Park, B.B., 2020. Cooperative Adaptive Cruise Control With Unconnected Vehicle in the Loop. IEEE Trans. Intell. Transp. Syst. PP (99), 1–11. https://doi.org/10.1109/TITS.2020.3041840.

Doyle, J.C., Francis, B.A., Tannenbaum, A.R., 2013. Feedback control theory. Courier Corporation.

Fukushima, H., Kim, T.H., Sugie, T., 2007. Adaptive model predictive control for a class of constrained linear systems based on the comparison model. Automatica 43 (2), 301–308. https://doi.org/10.1016/j.automatica.2006.08.026.

Ge, J.I., Orosz, G., 2018. Connected cruise control among human-driven vehicles: Experiment-based parameter estimation and optimal control design. Transp. Res. Part C Emerg. Technol. 95(August 2017), pp. 445–459, 2018, doi: 10.1016/j.trc.2018.07.021.

Ge, J.I., Orosz, G., 2014. Dynamics of connected vehicle systems with delayed acceleration feedback. Transp. Res. Part C Emerg. Technol. 46, 46–64. https://doi.org/10.1016/j.trc.2014.04.014.

Ge, J.I., Orosz, G., 2017. Optimal control of connected vehicle systems with communication delay and driver reaction time. IEEE Trans. Intell. Transp. Syst. 18 (8), 2056–2070. https://doi.org/10.1109/TITS.2016.2633164.

Ge, J.I., Avedisov, S.S., He, C.R., Qin, W.B., Sadeghpour, M., Orosz, G., 2018. Experimental validation of connected automated vehicle design among human-driven vehicles. Transp. Res. Part C 91, 335–352. https://doi.org/10.1016/j.trc.2018.04.005.

Ge, J.I., Orosz, G., 2017. Data-driven parameter estimation for optimal connected cruise control. In: 2017 IEEE 56th Annual Conference on Decision and Control, pp. 3739–3744. https://doi.org/10.1109/CDC.2017.8264208.

Gunter, G., Gloudemans, D., Stern, R.E., Mcquade, S., Work, D.B., 2020. Are commercially implemented adaptive cruise control systems string stable? IEEE Trans. Intell. Transp. Syst. PP(99), pp. 1–12.

Hasch, J., Topak, E., Schnabel, R., Zwick, T., Weigel, R., Waldschmidt, C., 2012. Millimeter-wave technology for automotive radar sensors in the 77 GHz frequency band. IEEE Trans. Microw. Theory Tech. 60 (3), 845–860. https://doi.org/10.1109/TMTT.2011.2178427.

- Jung, C., Lee, D., Lee, S., Shim, D.H., 2020. V2X-communication-aided autonomous driving: System design and experimental validation. Sensors 20 (10), 1–21. https://doi.org/10.3390/s20102903.
- Liu, H., Kan, X.(., Shladover, S.E., Lu, X.-Y., Ferlis, R.E., 2018. Modeling impacts of Cooperative Adaptive Cruise Control on mixed traffic flow in multi-lane freeway facilities. Transp. Res. Part C Emerg. Technol. 95, 261–279. https://doi.org/10.1016/j.trc.2018.07.027.
- Masini, B.M., Bazzi, A., Zanella, A., 2018. A survey on the roadmap to mandate on board connectivity and enable V2V-based vehicular sensor networks. Sensors (Switzerland) 18(7), doi: 10.3390/s18072207.
- Mehmood, A., Easa, S.M., 2009. Modeling reaction time in car-following behaviour based on human factors. Civ. Environ. Struct. Constr. Archit. Eng. 3 (9), 325–333. Milanes, V., Shladover, S.E., Spring, J., Nowakowski, C., Kawazoe, H., Nakamura, M., 2014. Cooperative adaptive cruise control in real traffic situations. IEEE Trans. Intell. Transp. Syst. 15 (1), 296–305. https://doi.org/10.1109/TITS.2013.2278494.
- Mobileye, "Our Technology Mobileye," 2021. https://www.mobileye.com/our-technology/ (accessed Jul. 06, 2021).
- Naus, G.J.L., Vugts, R.P.A., Ploeg, J., Van De Molengraft, M.J.G., Steinbuch, M., 2010. String-stable CACC design and experimental validation: A frequency-domain approach. IEEE Trans. Veh. Technol. 59 (9), 4268–4279. https://doi.org/10.1109/TVT.2010.2076320.
- Nieuwenhuijze, M.R.I., van Keulen, T., Öncü, S., Bonsen, B., Nijmeijer, H., 2012. Cooperative driving with a heavy-duty truck in mixed traffic: experimental results. IEEE Trans. Intell. Transp. Syst. 13 (3), 1026–1032. https://doi.org/10.1109/TITS.2012.2202230.
- Ploeg, J., Scheepers, B.T.M., van Nunen, E., van de Wouw, N., Nijmeijer, H., 2011. Design and experimental evaluation of cooperative adaptive cruise control. In: 2011 14th International IEEE Conference on Intelligent Transportation Systems (ITSC), pp. 260–265. https://doi.org/10.1109/ITSC.2011.6082981.
- Ploeg, J., Semsar-Kazerooni, E., Lijster, G., Van De Wouw, N., Nijmeijer, H., 2015. Graceful degradation of cooperative adaptive cruise control. IEEE Trans. Intell. Transp. Syst. 16 (1), 488–497. https://doi.org/10.1109/TITS.2014.2349498.
- Rajamani, R., Shladover, S.E., 2001. Experimental comparative study of autonomous and co-operative vehicle-follower control systems. Transp. Res. Part C Emerg. Technol. 9 (1), 15–31. https://doi.org/10.1016/S0968-090X(00)00021-8.
- Rakha, H.A., Ahn, K., Moran, K., Saerens, B., Van Den Bulck, E., 2011. Virginia tech comprehensive power-based fuel consumption model: model development and testing. Transp. Res. Part D 16 (7), 492–503. https://doi.org/10.1016/j.trd.2011.05.008.
- Shladover, S.E., 2018. Connected and automated vehicle systems: Introduction and overview. J. Intell. Transp. Syst. Technol. Planning, Oper. 22 (3), 190–200. https://doi.org/10.1080/15472450.2017.1336053.
- Shladover, S., et al., 2018. Cooperative Adaptive Cruise Control (CACC) For Partially Automated Truck Platooning: Final Report.
- Sugiyama, Y., Fukui, M., Kikuchi, M., Hasebe, K., Nakayama, A., Nishinari, K., Tadaki, S.-I., Yukawa, S., 2008. Traffic jams without bottlenecks—experimental evidence for the physical mechanism of the formation of a jam. New J. Phys. 10 (3), 033001. https://doi.org/10.1088/1367-2630/10/3/033001.
- Van Arem, B., Van Driel, C.J.G., Visser, R., 2006. The impact of cooperative adaptive cruise control on traffic-flow characteristics. IEEE Trans. Intell. Transp. Syst. 7 (4), 429–436. https://doi.org/10.1109/TITS.2006.884615.
- van Nunen, E., Kwakkernaat, M.R.J.A.E., Ploeg, J., Netten, B.D., 2012. Cooperative Competition for Future Mobility. IEEE Trans. Intell. Transp. Syst. 13 (3), 1018–1025. https://doi.org/10.1109/TITS.2012.2200475.
- Wei, S., Zou, Y., Zhang, T., Zhang, X., Wang, W., 2018. Design and experimental validation of a cooperative adaptive cruise control system based on supervised reinforcement learning. Appl. Sci. 8 (7), 1014. https://doi.org/10.3390/app8071014.
- Xiao, L., Gao, F., 2011. Practical string stability of platoon of adaptive cruise control vehicles. IEEE Trans. Intell. Transp. Syst. 12 (4), 1184–1194. https://doi.org/10.1109/TTS.2011.2143407.
- Xiao, L., Wang, M., Schakel, W., van Arem, B., 2018. Unravelling effects of cooperative adaptive cruise control deactivation on traffic flow characteristics at merging bottlenecks. Transp. Res. Part C Emerg. Technol. 96 (May), 380–397. https://doi.org/10.1016/j.trc.2018.10.008.
- Yang, H., Rakha, H., Ala, M.V., 2017. Eco-cooperative adaptive cruise control at signalized intersections considering queue effects. IEEE Trans. Intell. Transp. Syst. 18 (6), 1575–1585. https://doi.org/10.1109/TITS.2016.2613740.
- Zhang, L., Orosz, G., 2016. Motif-based design for connected vehicle systems in presence of heterogeneous connectivity structures and time delays. IEEE Trans. Intell. Transp. Syst. 17 (6), 1638–1651. https://doi.org/10.1109/TITS.2015.2509782.
- Zohdy, I.H., Kamalanathsharma, R.K., Rakha, H., 2012. Intersection management for autonomous vehicles using iCACC. IEEE Conf. Intell. Transp. Syst. Proceedings, ITSC, pp. 1109–1114, doi: 10.1109/ITSC.2012.6338827.